Chemical Science

ROYAL SOCIETY OF CHEMISTRY

EDGE ARTICLE

View Article Online
View Journal | View Issue

Cite this: *Chem. Sci.*, 2025, **16**, 18686

All publication charges for this article have been paid for by the Royal Society of Chemistry

Noncovalent immobilization of chiral Lewis acids on single-walled carbon nanotubes as a tool for synthetic organic aquachemistry

Taku Kitanosono, * Satoshi Tanaka, Dongxin Zhang, Tomoya Hisada, Yasuhiro Yamashita and Shu Kobayashi *

Polycyclic aromatic hydrocarbons (PAHs) were employed as anchoring tags to noncovalently immobilize Lewis acids onto single-walled carbon nanotubes (SWNTs). This heterogeneous system demonstrated remarkable performance in asymmetric catalysis, particularly in water devoid of organic solvents or surfactants, outperforming other carbonaceous π-materials in activity, stereoselectivity, and reusability. The use of large-diameter SWNTs modified with 4-fluorophenyl groups further enhanced catalytic activity. Notably, $Sc(PyS)_3$-SWNT combined with a chiral modifier retained high performance without the covalent anchorage, even after multiple reuse cycles. No leaching of scandium or the chiral modifier was observed, consistent with TGA results, despite washing with solvents in which the chiral modifier is highly soluble. XPS analysis demonstrated that among the supports examined, SWNTs exhibited the most significant electron donation to the Sc and S centers, underscoring the exceptional electronic interaction responsible for the stable immobilization. Despite its high surface area and adsorption capacity, activated carbon showed poor performance and significant leaching, suggesting that electron donation from SWNTs stabilizes flexible, solution-like conformations of the Lewis acid complex, mitigating the unavoidable attenuation of Lewis acidity more effectively than other supports. This strategy also mitigates deactivation risks posed by nucleophiles such as amines, thiols, and free N–H indoles, which typically displace chiral ligands. Thus, a robust, non-covalent immobilization platform has been established, capable of delivering high activity, selectivity, and durability even in water, which is traditionally challenging for Lewis acid catalysis. This approach offers a promising pathway toward more sustainable and environmentally conscious asymmetric synthesis.

Received 19th July 2025
Accepted 29th August 2025

DOI: 10.1039/d5sc05390k

rsc.li/chemical-science

Introduction

Among carbon allotropes, single-walled carbon nanotubes (SWNTs) have garnered multidisciplinary attention due to their unique properties, such as their quasi-one-dimensional nanostructure and exceptional electronic properties.[1] Despite their widespread use in physical and biological applications, their application in mainstream synthetic chemistry remains underexplored compared to other carbonaceous materials. This is surprising given their high mechanical strength, chemical stability, and large surface area, which make them appealing as support materials. To date, the use of SWNTs as catalyst supports has been sporadically reported in metal or metal oxide nanoparticle-catalyzed hydrogenation/dehydrogenation, oxidation/reduction, and Fischer–Tropsch reactions.[2]

In contrast, their application to single-ion catalysis remains scarce. Three strategies used so far include oxidative functionalization to introduce keto, carboxylate, aldehyde, and alcoholic fragments at the nanotube defect sites (Fig. 1a),[3] doping with heteroatoms (Fig. 1b),[4] and covalent/noncovalent immobilization of organometallic complexes (Fig. 1c).[5] The first two strategies are inadequate for fine organic synthesis due to ill-defined environments around metal ions and weak metal-anion interactions that may lead to metal leaching. In the latter examples, the potential of SWNTs remains underutilized as the active site is distant from the SWNT, despite the complex chemical synthesis involved. Furthermore, the electrochemical attribute of SWNTs has received scant attention in the field of organic synthesis, despite the importance of electronic effects in a vast number of chemical transformations and a long-standing interest in metal–support interactions.[6]

We have previously fabricated surfactant-based highly dispersed chiral nickel complex–SWNT composites for enantioselective synthesis with a minute quantity of defibrillated SWNTs (<25 mg SWNTs per mmol Ni^{2+}), wherein the electronic couplings between nickel(II) ions and SWNTs emerged as a linchpin for catalytic performance.[7] Nevertheless, the system was not designed with reusability in mind, owing to

Department of Chemistry, School of Science, The University of Tokyo, Bunkyo-ku, Tokyo, 113-0033, Japan. E-mail: tkitanosono@chem.s.u-tokyo.ac.jp; shu_kobayashi@chem.s.u-tokyo.ac.jp

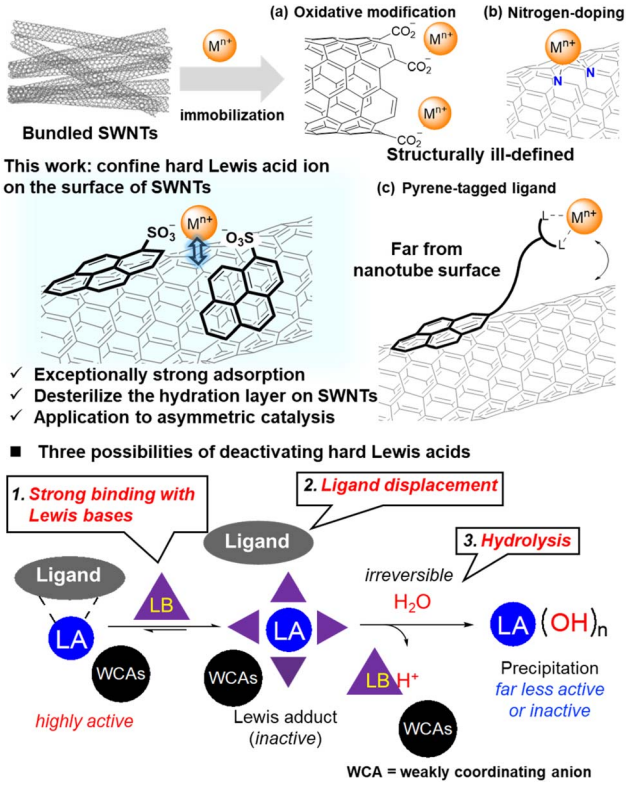

Fig. 1 Overview of concept and design.

the reliance on surfactants for SWNT dispersion. Eschewing the micelle-based paradigm, we herein disclose our endeavor to utilize SWNT bundles for catalyst immobilization, thereby enabling heterogenization of hard Lewis acid catalysis without covalent linkage (*ca.* 4–5 g SWNTs per mmol Lewis acid). Immobilizing Lewis acids onto solid supports remains a perennial conundrum in catalysis, particularly under aqueous conditions. Lewis acids are inherently prone to deactivation through strong binding with nucleophilic reactants, ligand displacement, or hydrolysis (Fig. 1). Moreover, their coordination environments are often perturbed upon immobilization, leading to diminished activity, selectivity, or leaching. Strong interactions with supports may also reduce the Lewis acidity. These challenges are further exacerbated when noncovalent strategies are employed, as the interactions between the metal center and the support are typically sensitive to reaction conditions. Other carbon-based materials such as carbon dots, carbon nitrides, and covalent organic frameworks (COFs) have been explored as supports for catalytic systems such as metal(0) or transition metals. However, their surface functionalities often include Lewis basic sites or polar groups that can coordinate to Lewis acids, thereby attenuating their acidity or causing deactivation. Furthermore, the electronic environments of these materials are typically less well-defined or tunable than those of SWNTs, rendering stable, noncovalent immobilization while preserving catalytic activity a formidable task. In contrast, SWNTs offer a hydrophobic, electronically rich, and structurally uniform surface that enables effective physisorption without compromising Lewis acidity, resulting in Goldilocks-level interactions, neither too strong nor too weak, with the SWNT surface. This feature not only facilitates catalyst regeneration during the reaction but also allows elegant modulation of the chiral environments, thereby broadening the applicability of the system across diverse catalytic transformations. Such a strategy may help dismantle both conceptual and practical barriers associated with noncovalent immobilization, which remains a formidable challenge. Moreover, the minimal degree of fixation enhances mass transfer, improving the diffusion of both substrates to and products from the active sites, thereby mitigating the performance drop often observed upon heterogenization. An aspirational goal of this project is to identify the unique capabilities of SWNTs as a support, capabilities that defy mimicry by other carbonaceous materials in organic synthesis. We envisaged the intrinsic electronic properties of SWNT bundles could play a decisive role in stably anchoring hydrated single metal ions that are often catalytically superior to their anhydrous counterparts, in conjunction with well-recognized advantages of SWNTs as support materials.[8] As discussed elsewhere, water molecules are known to form highly ordered structures on hydrophobic surfaces. Homma *et al.* reported the formation of a stable hydration layer on the surface of SWNTs through lateral hydrogen bonding, which is distinctly divergent from the behavior of bulk water.[9] This hydrated yet macroscopically hydrophobic layer may be effective for stable immobilization of whole "active microenvironments" composed of hydrated metal ions and structured water layers. In this context, synthetic organic aquachemistry,[10] a field that emphasizes organic synthesis in water without organic cosolvents or surfactants, offers a compelling paradigm: doing more with less.[11] The microenvironments embedded in the "hydrated yet macroscopically hydrophobic" surface layer of SWNT bundles could lead to efficient concentration of the reactants and amelioration in the diffusion.

Results and discussion

Catalyst development and evaluation

To noncovalently anchor single metal ions in proximity to SWNTs, we eschewed a linker-based approach, leveraging the well-documented high affinity[12] of pyrenyl groups for SWNTs (Fig. 1). Redox-inert scandium ions, featuring a d^0 electron configuration, were chosen to preclude any potential influence of metal ion redox properties on the adsorption. Unlike transition metals with partially filled d-orbitals, Sc^{3+} lacks d-electron-mediated effects such as ligand field stabilization or back-donation, making it a theoretically distinct case from our previous study.[7] This absence of d-electron interactions presents a unique challenge in achieving stable immobilization, as conventional mechanisms of electronic communication are unavailable. At the outset, the structurally simple scandium tris(pyrene-1-sulfonate) ($Sc(PyS)_3$) was synthesized from scandium oxide and pyrene-1-sulfonic acid, and its structure was confirmed by ^1H and ^{13}C NMR spectroscopy, as well as elemental analysis. UV-vis spectroscopy revealed that $Sc(PyS)_3$ has low solubility in water ($<1 \times 10^{-4}$ M; see the SI for the details). We then assessed the adsorption of $Sc(PyS)_3$ onto

various carbonaceous π-materials, including SWNTs (with a diameter of 1–2 nm), multi-walled carbon nanotubes (MWNTs), graphene nanoplatelets, and activated carbon (AC). Among these materials, SWNTs demonstrated the highest loading efficiency (0.190 mmol g^{-1}), while graphene nanoplatelets exhibited negligible adsorption of $Sc(PyS)_3$ (<0.01 mmol g^{-1}). This is because the higher effective curvature of SWNTs enhances the ion–π or π–π interactions due to localized electronic states, increased surface energy, and increased polarizability. Scanning transmission electron microscopy with energy dispersive spectroscopy (STEM-EDS) elemental mapping of the as-prepared $Sc(PyS)_3$–SWNT composite confirmed the uniform distribution of Sc^{3+} on the surface of SWNT bundles (Fig. S4). X-ray photoelectron spectroscopy (XPS) analysis was performed to investigate the interaction between $Sc(PyS)_3$ and the support materials. A significant redshift in both Sc and S binding energies was observed, providing compelling evidence for the electronic interaction between $Sc(PyS)_3$ and the supports. This shift indicates that the scandium center becomes electron-rich upon immobilization (Table S7), thereby leading to a discernible attenuation in Lewis acidity. The minimal dependence of peak shifts on the nature of the supports, coupled with the observation that sulfur becomes more electron-rich relative to scandium, suggests that the pyren-1-sulfonate anion engages in stronger and more intimate interactions with the π-surface of the supports. This can be rationalized by the fact that, unlike the cation–π interactions which occur exclusively between Sc^{3+} and SWNTs, the pyrene-1-sulfonate anion is robustly adsorbed onto SWNTs through both anion–π and π–π interactions. These electronic couplings underpin the robust immobilization *via* chemisorption concomitantly with decreased Lewis acidity. The catalytic activity of the prepared materials was benchmarked in a Nazarov-type reaction, where an oxyallyl cation is trapped by water to yield an α-diketone (Table 1). Interestingly, $Sc(PyS)_3$ alone exhibited comparable activity to a previously reported micellar catalyst system (entries 1 and 2).[13] Furthermore, notwithstanding decreased Lewis acidity, the use of SWNTs as a support for $Sc(PyS)_3$ led to superior catalytic performance compared to other supports (entries 3–5). This indicates that the active environments forged onto the surface of SWNTs are effective for organic reactions run in water.

Table 1 Nazarov-type reaction in water[c]

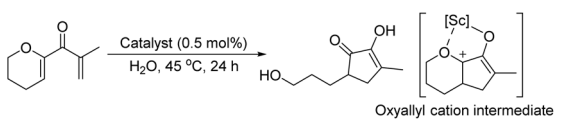

Entry	Catalyst	Yield[a] (%)
1	$Sc(DS)_3$	67 (16)[b]
2	$Sc(PyS)_3$	62 (14)[b]
3	$Sc(PyS)_3$–SWNT (0.190 mmol g^{-1})	87 (41)[b]
4	$Sc(PyS)_3$–MWNT (0.106 mmol g^{-1})	71
5	$Sc(PyS)_3$–AC (0.132 mmol g^{-1})	65

[a] Isolated yield. [b] Run with 0.25 mol% of catalyst. [c] $Sc(DS)_3$ = scandium tris(dodecylsulfate); $Sc(PyS)_3$ = scandium tris(pyrene-1-sulfonate); SWNT = single-walled carbon nanotube; MWNT = multi-walled carbon nanotube; AC = activated carbon.

Asymmetric variant

The observed superiority of SWNTs to other carbonaceous materials encouraged us to undertake the translation of SWNT-supported catalysis to asymmetric catalysis. Heterogenizing homogeneous chiral catalysts is an important strategy for manufacturing optically active substances, due to the ease of separation and recyclability of the catalyst from the post-reaction mixture. Although noncovalent immobilization of chiral complexes, without the need for complex synthesis of chiral ligand–support conjugates, is ideal for versatile applications, it is widely recognized as a significant challenge in the field compared to common covalent immobilization. The oft-observed deteriorated outcomes in unsuccessful examples are primarily attributable to leaching issues, which are highly dependent on the reaction conditions, immobilization methods, supports, and the chiral complexes themselves.[14] This highlights a fundamental limitation of non-covalent immobilization strategies—namely, their limited tolerance to variations in these parameters. Additionally, the use of Lewis basic reactants notoriously reduces activity persistence within a few runs,[5b,15,16] and the general solution is to adopt rigorously anhydrous conditions, sometimes accompanied by a reactivation process.[17] To further complicate matters, when nucleophiles, which are Lewis bases, are present in excess relative to the chiral Lewis acid catalyst, the chiral modifiers are easily dislodged from the Lewis acid unless covalently supported. This occurs because the chiral Lewis acid catalysts rely on Lewis acid–base interactions between the Lewis acid site and the chiral ligand. Consequently, recovering and reusing the chiral complexes, which are only interacting through noncovalent bonds, is challenging.

To our delight, a mixture of solids, comprising supported $Sc(PyS)_3$ and chiral 2,2′-bipyridine **L**,[18] formed the desired self-assemblies that enantioselectively catalyze the ring-opening reaction of meso-epoxide with aniline when stirred in water (Fig. 2), despite their poor solubility in water. This solid–solid self-assembly is similar to several examples[19–22] that have emerged in synthetic organic aquachemistry.[10a] Notably, the reaction hardly proceeded in organic solvents such as dichloromethane, diethyl ether, and tetrahydrofuran, even with a three-fold increase in the amount of $Sc(PyS)_3$, regardless of whether it dissolved or not. These outcomes are somewhat surprising given that $Sc(OTf)_3$ exhibited excellent reactivity in dichloromethane.[23] Although the decreased Lewis acidity of $Sc(PyS)_3$, as supported by XPS studies (Table S7), may account for the lack of activity in organic solvents, the good catalytic activity observed exclusively in water may be attributed to the partial dissociation of the counterion through hydration. This also supports the concept of exploiting SWNTs as a hydrated yet macroscopically hydrophobic layer. The strength of the interaction between Sc^{3+} and the SWNT surface is likely modulated

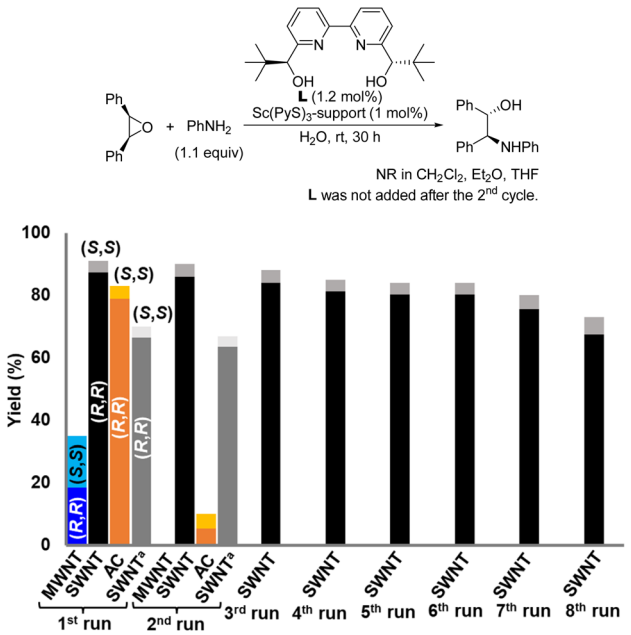

Fig. 2 Effect of carbonaceous materials on recyclability of chiral catalysts in water. [a] $Sc(OSO_3C_{12}H_{25})_3$ was used instead of $Sc(PyS)_3$.

by multiple parameters, including the nanotube curvature, chirality, and specific immobilization geometry of the scandium complex. Given that SWNTs are inherently a mixture of numerous structural variants, it is reasonable to interpret the observed catalytic activity as the ensemble average of a broad distribution of stable and metastable immobilization states.

While $Sc(PyS)_3$–SWNT and $Sc(PyS)_3$–AC provided more than 90% ee of the desired β-amino alcohol in high yield, $Sc(PyS)_3$–MWNTs exhibited slower reaction kinetics and yielded an almost racemic product. This suggests suboptimal coordination of the chiral modifier **L** to the supported scandium ion, potentially attributable to the limited accessibility of solid **L** to scandium ions entrenched within the entangled fibrous network of MWNTs. Both SWNT- and AC-supported catalysts were readily separable from the post-reaction mixture *via* simple filtration. Impressively, the catalytic performance of the reused SWNT-supported catalyst was retained in the second run, even without adding additional **L**. This is somewhat surprising because **L** is highly soluble in ethyl acetate, the solvent used during the washing process. Conversely, the use of AC as a support led to pronounced deactivation of the catalyst. Elemental analysis of recovered catalysts following the first run revealed that both Sc^{3+} and the chiral modifier were nearly quantitatively retained in the SWNT-supported system, whereas approximately 50% of Sc^{3+} content and >95% of **L** were lost in the AC-supported catalyst. This finding is especially noteworthy, considering that AC is widely used as a superior support due to its high surface area, excellent dispersibility, and strong adsorption capacity. Although SWNTs do not boast the highest surface area, the best dispersibility, or the strongest adsorption capacity among the carbonaceous supports examined, none of the alternative supports succeeded in mitigating leaching, which invariably led to substantial losses in both catalytic activity and enantioselectivity. These comparative insights strongly suggest that the exceptional performance of the SWNT-supported catalyst cannot be ascribed to the general physical properties of the support alone. Rather, we posit that the crucial determinant lies in the electronic interaction between the Sc^{3+} center and the SWNT surface. The XPS data presented in Table S7 currently stand as the only analytical evidence distinguishing SWNTs from other carbon supports in this context. Given that such electron donation would naturally engender stronger binding of the metal center to the support, it offers a plausible, rational, and empirically grounded explanation for the observed suppression of leaching.

Remarkably, the SWNT-supported catalyst was successfully reused for eight consecutive cycles without the addition of **L**. The Sc content showed no decrease even after the 8th run, while 7% of **L** was lost. While the unmodified $Sc(PyS)_3$ exhibited negligible catalytic activity, $Sc(PyS)_3$-SWNT demonstrated a modicum of activity (Table S8). Consequently, the inevitable reduction of the chiral modifier leads to a concomitant decline in both catalytic activity and selectivity. This not only indicates that the observed slight decrease in yield and enantioselectivity upon reuse is due to the loss of **L**, but also emphasizes that more than 93% of Sc^{3+} remained bound to **L**, underscoring the efficiency of this noncovalent immobilization method. Additionally, the use of scandium tris(dodecyl sulfate) $Sc(DS)_3$ instead of $Sc(PyS)_3$ led to 37% leaching of Sc^{3+}, despite almost fully retaining catalytic activity in the 2nd run. This suggests the importance of the pyrenyl moiety for confining Sc^{3+} on the surface of SWNTs, and the non-involvement of the pyrenyl moiety in immobilizing **L**.

The unique properties of SWNTs in noncovalently immobilized asymmetric catalysis have yet to be fully appreciated in terms of versatility and practicality. Several variables make it difficult to fully understand the effect of the physicochemical properties of SWNTs, including manufacturing methods, lot-to-lot variability, chirality of the structure, and so on. Attention then turned to large-diameter SWNTs, which are less susceptible to these factors due to their increased oxidation potential resulting from a bandgap reduction.[24] However, while physicochemical properties reach a plateau, increased oxidation potential may weaken the interaction between $Sc(PyS)_3$ and SWNTs and stabilize SWNT agglomeration. Although the technique could be applied to large-diameter SWNTs (3–5 nm), the $Sc(PyS)_3$-SWNT composite inevitably suffered from far inferior performance (43% yield). Notably, agglomeration significantly hindered stirring during the reaction, which may have contributed to the low catalytic efficiency. The SWNTs produced with the super-growth method[25] (ZEONANO® SG101) were used hereafter and displayed traits including a higher aspect ratio, higher purity (especially metal impurities), and larger surface area than SWNTs prepared with other methods, along with large diameter.

Arylation of the SWNT surface to improve catalytic activity

To address the challenge of agglomeration, three primary functionalization techniques exist: covalent, noncovalent, and

solvent exfoliation.[26] Due to the unsuitability of the latter two for catalyst immobilization and recovery, we pursued a covalent functionalization approach. Utilizing the Gomberg–Bachmann reaction with aryl diazonium salts, we aimed to improve SWNT dispersibility. This approach could introduce additional interactions such as π–π, C–H/π, and halogen−π, potentially enhancing the adsorption of species like $Sc(PyS)_3$, and the utility of aryl diazonium salts has led to the exploration of surfactant-based[27] and non-aqueous methods[28] (employing isoamyl nitrite and aniline). While the detailed mechanism remains under debate, recent studies suggest a preferential reaction with metallic SWNTs over semiconducting ones through a radical mechanism,[29] chirality dependence,[30] and faster kinetics for larger diameter SWNTs.[31,32] Because it is theoretically contemplated that the presence of a band gap in semiconducting SWNTs results in a robust interaction with the chiral scandium complex, rather than with metallic SWNTs, the preferential reaction of metallic SWNTs with the aryl radical would minimize the effect of undesired interactions. In light of these findings, we evaluated three methods for introducing the 4-fluorophenyl functionality, assessing them based on fluorine loading efficiency (Table S3). The surfactant-based method exhibited lower loading and efficiency, along with surfactant contamination. The use of a solution of 4-fluorobenzene diazonium tetrafluoroborate ($4\text{-}FC_6H_4N_2BF_4$) in acetonitrile proved optimal. A two-step weight loss observed in thermogravimetric analysis (TGA) supports the presence of a covalently linked functionality, consistent with previous reports (Fig. S5).[33] Furthermore, X-ray photoelectron spectroscopy (XPS) analysis revealed the F 1s peak associated with the C–F bond underwent a blue shift compared to $4\text{-}FC_6H_4N_2BF_4$ (Fig. S6) and no boron was detected in the digested sample *via* inductively coupled plasma optical emission spectroscopy (ICP-OES). These outcomes are consistent with the formation of the Gomberg–Bachmann product of SWNTs.

As shown in Fig. 3, subsequent to arylation with $R\text{–}C_6H_4N_2BF_4$, a stepwise treatment with $Sc(PyS)_3$ and **L** yielded the composite **L**$Sc(PyS)_3$–SWNT(R). The arylated catalyst (R = F) demonstrated enhanced dispersibility during the ring-opening reaction in water (Fig. 3a). UV-vis spectroscopy of the solution proved valuable for real-time monitoring of aryl diazonium tetrafluoroborate consumption, aligning with NMR analysis results. The degree of functionalization could be controlled by adjusting the incubation time, monitored *via* UV-vis spectroscopy. Functionalization was negligible below 0.2 mmol g^{-1}, but the reaction rate increased significantly within the range of 0.2–0.4 mmol g^{-1}, with 0.32 mmol g^{-1} proving optimal (Fig. 3b). XPS spectra of highly arylated SWNTs (0.479 mmol g^{-1} F^{-1} loading) revealed an N 1s peak at 400 eV, attributed to the diazo C–N═N–C linkage. This suggests that excessive arylation might reduce the Lewis acidity of Sc^{3+} through undesired interactions with this linkage. Notably, the uniform redshift in the binding energy (BE) of Sc $2p^{1/2}$, $2p^{3/2}$, and N 1s peaks upon being supported on SWNTs corroborates electron donation from SWNTs to the scandium complex (Fig. S8). The minute peak blueshift with uniformity by surface arylation may be attributed to the electron-withdrawing property of the 4-fluorophenyl group.

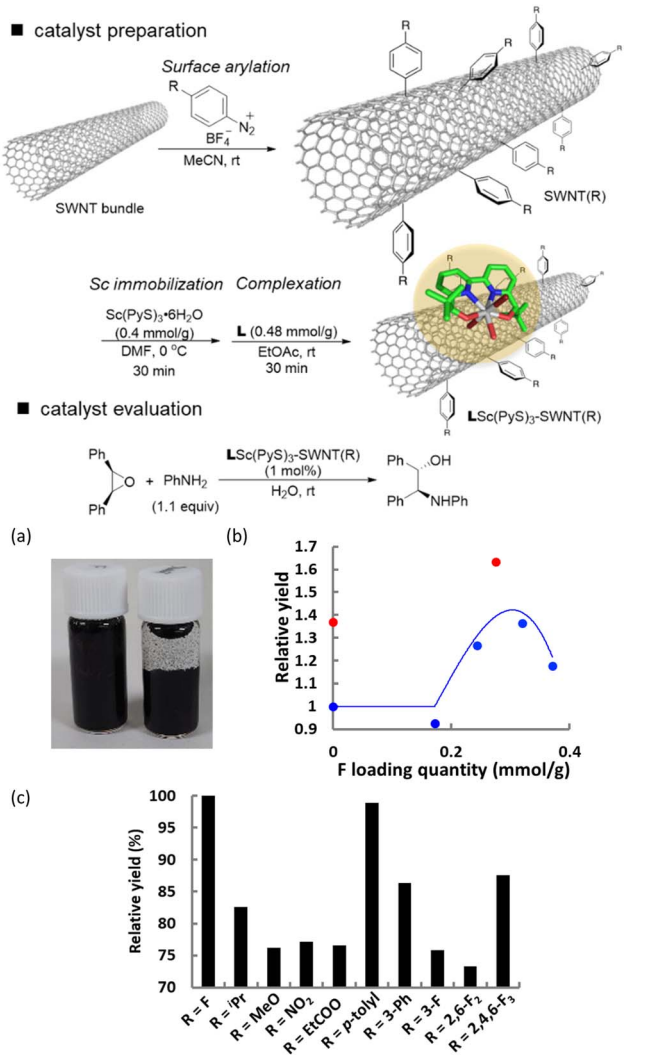

Fig. 3 Arylation of the SWNT surface: (a) appearance of the reaction mixture [right: unmodified SWNT-based catalyst LSc(PyS)$_3$–SWNT, left: arylated SWNT-based catalyst LSc(PyS)$_3$–SWNT(F)]; (b) effect of the loading quantity of the 4-fluorophenyl moiety for Sc(PyS)$_3$ (blue) and Sc(^{t}BuPyS)$_3$ (red); (c) effect of substituents. The product yield of the major (*S,S*) isomer was used.

Subsequently, the SWNTs were arylated with various substituted aryldiazonium tetrafluoroborate compounds, targeting a functionalization degree of 0.3–0.4 mmol g^{-1}. In some cases, the actual degree of functionalization deviated due to byproduct formation. For instance, nitrobenzene was produced to some extent in the reaction with 4-nitrobenzene diazonium tetrafluoroborate, consistent with the documented radical-involved mechanism. A summary of this study is presented in Fig. 3c and S2. Electronically neutral substituents resulted in higher yields, indicating that the Lewis acidity of Sc^{3+} is influenced by the electronic nature of the SWNT surface. Ultimately, the installation of a 4-fluorophenyl group proved optimal. Aryl radicals bearing electron-donating substituents at the 4-position (OMe, ^{i}Pr) may competitively react with electron-deficient semiconducting SWNTs, leading to decreased Lewis acidity and decreased reaction yield. In addition, electron-donating

substituents may promote the growth of the aryl layer by the formation of a polyphenylene-like layer. In contrast, electron-withdrawing substituents (NO_2, CO_2Et) at the 4-position of the aryl radical may inhibit an undesired reaction with semiconducting SWNTs and the growth of the aryl layer, but result in decreased catalytic activity by their coordination to the scandium ion. Substitution at the 4-position, which is the most reactive for a radical addition reaction, seems to be important for high catalytic performance. Notably, Sc^{3+} leaching was not observed, even when supported on arylated SWNTs.

The π–π interactions between pyrenyl moieties can induce proximity or lamination of Sc^{3+} on the SWNT surface, potentially diminishing catalytic activity and robustness. To ameliorate this, several scandium salts bearing polycyclic aromatic hydrocarbons (PAHs) in their counteranion were prepared. Fortuitously, the use of scandium tris[(7-*tert*-butyl)pyrene-1-sulfonate], Sc(^{t}BuPyS)$_3$, significantly enhanced catalytic activity, albeit with no dependence of enantioselectivity to the tag structure (Table S9). The triphenylene-2-sulfonate (TPhS), likely to display higher binding affinity than pyrene[12] presumably due to its larger molecular volume,[34] also exhibited commendable catalytic performance. Under these optimized conditions, the catalyst could be reused up to 10 times without any leaching of Sc^{3+} ions (Fig. 4a). Contrary to the observations in Fig. 2, no decline in catalytic activity was noted with repeated use, although enantioselectivity was subtly eroded. The sustained activity may be attributed to the addition of the chiral modifier and the employment of large-diameter SWNTs. Remarkably, the loss of the chiral modifier during filtration and washing was minimized, resulting in only a very gradual decline in enantioselectivity. In TGA of the catalyst before and after the reaction (Fig. S11), the endpoint remained ostensibly unaltered even subsequent to the first run, corroborating the experimental outcomes of no leaching of both organic and inorganic materials. XPS analysis revealed that the catalyst recovered after the 10th run underwent subtle changes with no clear decrease in the Lewis acidity of the catalyst (Fig. S10), possibly attributable to the changes in the morphology of the SWNT agglomerations. This is in sharp contrast to a polystyrene-bound chiral scandium catalyst,[16] which exhibited decreased Lewis acidity with repeated reuse in XPS analysis. While the structure of the scandium complex in an immobilized state can modulate the Lewis acidity and enantioselectivity, deciphering these effects at the molecular level remains an immense challenge. While the structure of the scandium complex in an immobilized state can modulate the Lewis acidity and enantioselectivity, deciphering these effects at the molecular level remains an immense challenge.

With optimal conditions in hand, the substrate scope was explored, as depicted in Fig. 4b. A diverse range of *N*-nucleophiles (anilines), irrespective of the electronic nature of the substituents, *O*-nucleophile (4′-bromobenzyl alcohol), *S*-nucleophile (4-methoxybenzenethiol), and free *N*-H indole, notwithstanding their notorious catalyst-poisoning capability, were successfully employed, affording optically active β-amino

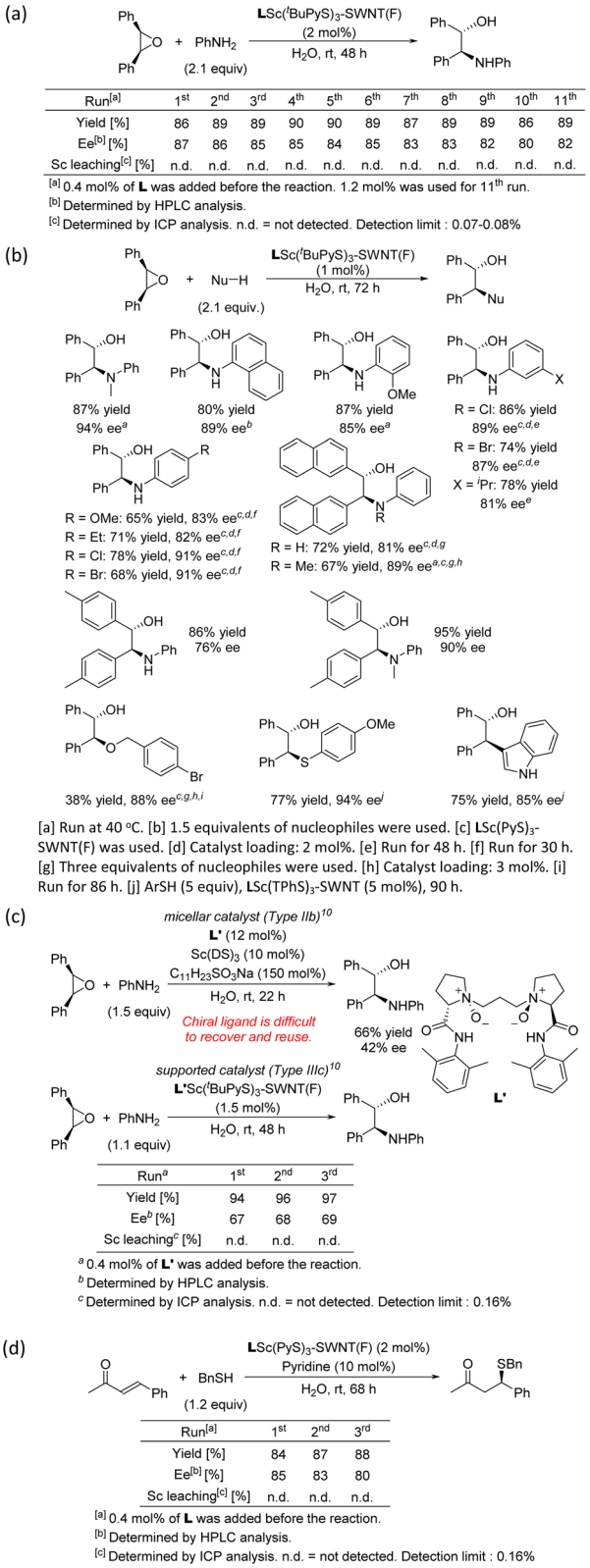

Run[a]	1st	2nd	3rd	4th	5th	6th	7th	8th	9th	10th	11th
Yield [%]	86	89	89	90	90	89	87	89	89	86	89
Ee[b] [%]	87	86	85	85	84	85	83	83	82	80	82
Sc leaching[c] [%]	n.d.	n.d.	n.d.	n.d.	n.d.	n.d.	n.d.	n.d.	n.d.	n.d.	n.d.

[a] 0.4 mol% of **L** was added before the reaction. 1.2 mol% was used for 11th run.
[b] Determined by HPLC analysis.
[c] Determined by ICP analysis. n.d. = not detected. Detection limit : 0.07-0.08%

87% yield, 94% ee[a]
80% yield, 89% ee[b]
87% yield, 85% ee[a]
R = Cl: 86% yield, 89% ee[c,d,e]
R = Br: 74% yield, 87% ee[c,d,e]
X = ^{i}Pr: 78% yield, 81% ee[e]
R = OMe: 65% yield, 83% ee[c,d,f]
R = Et: 71% yield, 82% ee[c,d,f]
R = Cl: 78% yield, 91% ee[c,d,f]
R = Br: 68% yield, 91% ee[c,d,f]
R = H: 72% yield, 81% ee[c,d,g]
R = Me: 67% yield, 89% ee[a,c,g,h]
86% yield, 76% ee
95% yield, 90% ee
38% yield, 88% ee[c,g,h,i]
77% yield, 94% ee[j]
75% yield, 85% ee[j]

[a] Run at 40 °C. [b] 1.5 equivalents of nucleophiles were used. [c] LSc(PyS)$_3$-SWNT(F) was used. [d] Catalyst loading: 2 mol%. [e] Run for 48 h. [f] Run for 30 h. [g] Three equivalents of nucleophiles were used. [h] Catalyst loading: 3 mol%. [i] Run for 86 h. [j] ArSH (5 equiv), LSc(TPhS)$_3$-SWNT (5 mol%), 90 h.

Run[a]	1st	2nd	3rd
Yield [%]	94	96	97
Ee[b] [%]	67	68	69
Sc leaching[c] [%]	n.d.	n.d.	n.d.

[a] 0.4 mol% of **L'** was added before the reaction.
[b] Determined by HPLC analysis.
[c] Determined by ICP analysis. n.d. = not detected. Detection limit : 0.16%

Run[a]	1st	2nd	3rd
Yield [%]	84	87	88
Ee[b] [%]	85	83	80
Sc leaching[c] [%]	n.d.	n.d.	n.d.

[a] 0.4 mol% of **L** was added before the reaction.
[b] Determined by HPLC analysis.
[c] Determined by ICP analysis. n.d. = not detected. Detection limit : 0.16%

Fig. 4 Scope of reactions: (a) recovery and reuse experiments. (b) Scope of substrates. (c) Effect of chiral modifiers on recyclability. (d) Thia-Michael addition using Sc(^{t}BuPyS)$_3$–SWNT and **L**.

alcohols in commendable yields. Our noncovalent anchoring strategy hinges upon the interactions between $Sc(PyS)_3$ and SWNTs, rather than those between ligands and SWNTs. Hence, substituting one chiral modifier for another may highlight the ease with which the chiral modifier can be tuned. To substantiate this, we assessed the impact of the chiral modifier (Fig. 4c). The use of chiral *N*,*N*′-dioxide **L**′ [35] that possesses a tetradentate N_2O_2 donor akin to **L** exhibited moderate enantioselectivity (42% ee) under optimized micellar conditions, where **L**′ cannot be recycled without an extraction–chromatographic separation process. In contrast, the reaction using $Sc(^tBuPyS)_3$-SWNT(F) proceeded more selectively with lower catalyst loading. Given the unsupported catalyst exhibited a selectivity of 43%, comparable to the micelle catalyst system, the support on SWNTs evidently enhanced enantioselectivity. Furthermore, the catalyst, along with **L**′, could be recycled without erosion of enantioselectivity. This outcome indicates that our strategy is not confined to a particular chiral modifier, and increased enantioselectivity may indicate that the complex with **L**′ is immobilized in a more robust coordination manner than that with **L**. That is, the retained reusability of the catalyst even when the chiral modifier is altered represents an important and practical advantage. The observed enhancement in enantioselectivity upon immobilization suggests improved complex stability, further underscoring the benefits of our approach.

To further validate the robustness of the catalyst, the scandium-catalyzed thia-Michael addition[36] using an excessive quantity of pyridine relative to scandium was implemented (Fig. 4d). Pyridine is conceived to be sufficiently competent to displace a chiral modifier from the scandium ion and to deactivate the scandium ion through hydrolysis: nonetheless, the catalyst could be recycled while retaining a high level of enantioselectivity.

Conclusions

This study highlights the strategic prowess of SWNTs as a support platform for advancing organic synthesis in water. Polycyclic aromatic hydrocarbon (PAH)-based anions served as effective anchoring motifs, enabling the noncovalent yet tenacious immobilization of hard Lewis acids, including chiral variants, onto the SWNT surface, even in the absence of covalent linkage of the chiral modifier. This design not only suppressed Sc^{3+} leaching but also preserved catalytic performance across multiple cycles in asymmetric ring-opening reactions and thia-Michael addition that are run in water. Strikingly, the system retained its stability even in the presence of excess Lewis bases, which are typically both potent catalyst poisons and solvents for the chiral modifier. Given the inherent vulnerability of hard Lewis acids to hydrolysis and ligand displacement, especially in aqueous and basic environments, their stable immobilization without covalent tethering has long remained a formidable challenge. Our findings demonstrate that SWNTs, by virtue of their distinctive electronic and interfacial attributes, can overcome these limitations, offering a robust platform for noncovalent anchoring of hard Lewis acids. We posit this underlying design principle is broadly applicable to a wide array of metal-ion-catalyzed asymmetric reactions. As such, it offers a compelling blueprint for streamlining synthetic organic chemistry, in harmony with the tenets of green and sustainable chemistry.

Author contributions

T. K. and S. K. conceived the idea and were in charge of overall direction and planning. D. Z., T. H., and S. T. performed the experiments. T. K. took the lead in the interpretation of the results and in writing the manuscript.

Conflicts of interest

There are no conflicts to declare.

Data availability

The data supporting this article have been included as part of the SI.

Supplementary information: Experimental details; optimization details; characterization data; control experiments; computational studies. See DOI: **https://doi.org/10.1039/d5sc05390k**.

Acknowledgements

This work was supported by Grants-in-Aid for Science Research (JP19H05288, JP20K15272, and JP25K08633 to TK, and JP22H04972 to TK, YY, and SK) from the Japan Society for the Promotion of Science (JSPS). We also thank Dr Tei Maki (The University of Tokyo and JEOL Ltd) for STEM analyses. We acknowledge Dr Janet Bahri and Mr Akihiro Ide for their engagement during the early stage of this work.

References

1 (*a*) S. Iijima and T. Ishihashi, Single-shell carbon nanotubes of 1-nm diameter, *Nature*, 1993, **363**, 603–605; (*b*) D. S. Bethune, C. H. Kiang, M. S. DeVries, G. Gorman, R. Savoy and R. Beyers, Cobalt-catalysed growth of carbon nanotubes with single-atomic-layer walls, *Nature*, 1993, **363**, 605–607.

2 (*a*) V. Lordi, N. Yao and J. Wei, Method for supporting platinum on single-walled carbon nanotubes for a selective hydrogenation catalyst, *Chem. Mater.*, 2001, **13**, 733–737; (*b*) G. Wu, Y.-S. Chen and B.-Q. Xu, Remarkable support effect of SWNTs in Pt catalyst for methanol electrooxidation, *Electrochem. Commun.*, 2005, **7**, 1237–1243; (*c*) W. Shi, B. Zhang, Y. Lin, Q. Wang, Q. Zhang and D. S. Su, Enhanced chemoselective hydrogenation through tuning the interaction between Pt nanoparticles and carbon supports: insights from identical location transmission electron microscopy and X-ray photoelectron spectroscopy, *ACS Catal.*, 2016, **6**, 7844–7854; (*d*) A. H. Labulo, B. S. Martincigh, B. Omondi and V. O. Nyamori, Advances in carbon nanotubes as

efficacious supports for palladium-catalysed carbon-carbon cross-coupling reactions, *J. Mater. Sci.*, 2017, **52**, 9225–9248; (*e*) R. Dubey, D. Dutta, A. Sarkar and P. Chattopadhyay, Functionalized carbon nanotubes: synthesis, properties and applications in water purification, drug delivery, and material and biomedical sciences, *Nanoscale Adv.*, 2021, **3**, 5722–5744; (*f*) Y. Rangraz and M. M. Heravi, Recent advances in metal-free heteroatom-doped carbon heterogeneous catalysts, *RSC Adv.*, 2021, **11**, 23725–23778.

3 S. Banerjee and S. S. Wong, Functionalization of carbon nanotubes with a metal-containing molecular complex, *Nano Lett.*, 2002, **2**, 49–53.

4 Q. Ding, Y. Yu, F. Huang, L. Zhang, J.-G. Zheng, M. Xu, J. B. Baell and H. Huang, A reusable CNT-supported single-atom iron catalyst for the highly efficient synthesis of C–N bonds, *Chem.–Eur. J.*, 2020, **26**, 4592–4598.

5 (*a*) F. J. Gómez, R. J. Chen, D. Wang, R. M. Waymouth and H. Dai, Ring opening metathesis polymerization on non-covalently functionalized single-walled carbon nanotubes, *Chem. Commun.*, 2003, 190–191; (*b*) D. Didier and E. Schulz, π-Stacking interactions at the service of [Cu]-bis(oxazoline) recycling, *Tetrahedron: Asymmetry*, 2013, **24**, 769–775.

6 (*a*) C. E. Hamilton, D. Ogrin, L. McJilton, V. C. Moore, R. Anderson, R. E. Smalley and A. R. Barron, Functionalization of SWNTs to facilitate the coordination of metal ions, compounds and clusters, *Dalton Trans.*, 2008, 2937–2944; (*b*) F. Banhart, Interactions between metals and carbon nanotubes: at the interface between old and new materials, *Nanoscale*, 2009, **1**, 201–213; (*c*) J. Chen, Y. Zhang, Z. Zhang, D. Hou, F. Bai, Y. Han, C. Zhang, Y. Zhang and J. Hu, Metal-support interactions for heterogeneous catalysis: mechanisms, characterization techniques and applications, *J. Mater. Chem. A*, 2023, **11**, 8540–8572.

7 T. Kitanosono, P. Xu and S. Kobayashi, Chiral Lewis acids integrated with single-walled carbon nanotubes for asymmetric catalysis in water, *Science*, 2018, **362**, 311–315.

8 (*a*) D. J. Averill, P. Dissanayake and M. J. Allen, The Role of Water in Lanthanide-Catalyzed Carbon-Carbon Bond Formation, *Molecules*, 2012, **17**, 2073–2081; (*b*) M. Hatanaka and K. Morokuma, Role of Water in Mukaiyama-Aldol Reaction Catalyzed by Lanthanide Lewis Acid: A Computational Study, *J. Am. Chem. Soc.*, 2013, **135**, 13972–13979.

9 Y. Homma, S. Chiashi, T. Yamamoto, K. Kono, D. Matsumoto, J. Shitaba and S. Sato, Photoluminescence measurements and molecular dynamics simulations of water adsorption on the hydrophobic surface of a carbon nanotube in water vapor, *Phys. Rev. Lett.*, 2013, **110**, 157402.

10 (*a*) T. Kitanosono and S. Kobayashi, Synthetic organic "aquachemistry" that relies on neither cosolvents nor surfactants, *ACS Cent. Sci.*, 2021, **7**, 739–747; (*b*) T. Kitanosono and S. Kobayashi, Reactions in water involving the "on-water" mechanism, *Chem.–Eur. J.*, 2020, **26**, 9408–9429.

11 (*a*) S. B. Kim, B. J. Koo, S. B. Lee, W. H. Kim and H. Y. Bae, Water-enhanced catalysis: A broadly applicable strategy for promoting reactivity and selectivity in diverse chemical reactions, *Acc. Chem. Res.*, 2025, **58**, 1997–2015; (*b*) G. Anikumar, N. A. Harry and S. M. Ujwaldev, *Organic Transformations in Water: Principles and Applications*, Wiley-VCH, 2025; (*c*) T. Kitanosono, K. Masuda, P. Xu and S. Kobayashi, Catalytic organic reactions in water toward sustainable society, *Chem. Rev.*, 2018, **118**, 679–746.

12 (*a*) J. T. Yoo, T. Fujigaya and N. Nakashima, Molecular recognition at the nanoscale interface within carbon nanotube bundles, *Nanoscale*, 2013, **5**, 7419–7424; (*b*) J. T. Yoo, H. Ozawa, T. Fujigaya and N. Nakashima, Evaluation of affinity of molecules for carbon nanotubes, *Nanoscale*, 2011, **3**, 2517–2522.

13 M. Kokubo and S. Kobayashi, Nazarov-type reactions in water, *Chem.–Asian J.*, 2009, **4**, 526–528.

14 J. M. Fraile, J. I. García and J. A. Mayoral, Noncovalent immobilization of enantioselective catalysts, *Chem. Rev.*, 2009, **109**, 360–417.

15 (*a*) Y. Wan, P. McMorn, F. E. Hancock and G. J. Hutchings, Heterogeneous enantioselective synthesis of a dihydropyran using Cu-exchanged microporous and mesoporous materials modified by bis(oxazoline), *Catal. Lett.*, 2003, **91**, 145–148; (*b*) T. Ogawa, N. Kumagai and M. Shibasaki, Self-assembling neodymium/sodium heterobimetallic asymmetric catalyst confined in a carbon nanotube network, *Angew. Chem., Int. Ed.*, 2013, **52**, 6196–6201.

16 For heterogeneous asymmetric catalysis run in water with the covalent immobilization technique, see:T. Kitanosono, F. Lu, K. Masuda, Y. Yamashita and S. Kobayashi, Efficient recycling of catalyst-solvent couples from Lewis acid catalyzed asymmetric reactions in water, *Angew. Chem., Int. Ed.*, 2022, **61**, e202202335.

17 (*a*) K. Hashimoto, N. Kumagai and M. Shibasaki, A carbon nanotube confinement strategy to implement homogeneous asymmetric catalysis in the solid phase, *Chem.–Eur. J.*, 2015, **21**, 4262–4266; (*b*) H. Ishitani, K. Kanai, W.-J. Yoo, T. Yoshida and S. Kobayashi, A nickel-diamine/mesoporous silica composite as a heterogeneous chiral catalyst for asymmetric 1,4-addition reactions, *Angew. Chem., Int. Ed.*, 2019, **58**, 13313–13317; (*c*) Y. Saito and S. Kobayashi, Chiral heterogeneous scandium Lewis acid catalysts for continuous-flow enantioselective Friedel-Crafts carbon-carbon bond-forming reactions, *Angew. Chem., Int. Ed.*, 2022, **60**, 26566–26570.

18 C. Bolm, M. Zehnder and D. Bur, Optically active bipyridines in asymmetric catalysis, *Angew. Chem., Int. Ed.*, 1990, **29**, 205–207.

19 (*a*) S. Kobayashi, P. Xu, T. Endo, M. Ueno and T. Kitanosono, Chiral copper(II)-catalyzed enantioselective boron conjugate additions to α,β-unsaturated carbonyl compounds in water, *Angew. Chem., Int. Ed.*, 2012, **51**, 12763–12766; (*b*) T. Kitanosono, P. Xu, S. Isshiki, L. Zhu and S. Kobayashi, Cu(II)-catalyzed asymmetric boron conjugate addition to α,β-unsaturated imines in water, *Chem. Commun.*, 2014,

50, 9336–9339; (*c*) T. Kitanosono, P. Xu and S. Kobayashi, Heterogeneous versus homogeneous copper(II) catalysis in enantioselective conjugate addition reactions of boron in water, *Chem.–Asian J.*, 2014, **9**, 179–188.

20 T. Kitanosono and S. Kobayashi, Asymmetric boron conjugate additions to enones in water catalyzed by copper(0), *Asian J. Org. Chem.*, 2013, **2**, 961–966.

21 M. Ueno, A. Tanoue and S. Kobayashi, Catalytic organic reactions on the surface of silver(I) oxide in water, *Chem. Lett.*, 2014, **43**, 1867–1869.

22 T. Kitanosono, T. Hisada, Y. Yamashita and S. Kobayashi, Water-driven solid self-assembled catalysis, *J. Organomet. Chem.*, 2022, **965–966**, 122318.

23 (*a*) M. Kokubo, T. Naito and S. Kobayashi, Chiral zinc(II) and copper(II)-catalyzed asymmetric ring-opening reactions of *meso*-epoxides with aniline and indole derivatives, *Tetrahedron*, 2010, **66**, 1111–1118; (*b*) S. Azoulay, K. Manabe and S. Kobayashi, Catalytic Asymmetric Ring Opening of *meso*-Epoxides with Aromatic Amines in Water, *Org. Lett.*, 2005, **7**, 4593–4595.

24 Y. Hirana, G. Juhasz, Y. Miyauchi, S. Mouri, K. Matsuda and N. Nakashima, Empirical prediction of electronic potentials of single-walled carbon nanotubes with a specific chirality (n, m), *Sci. Rep.*, 2013, **3**, 2959.

25 K. Hata, D. N. Futaba, K. Mizuno, T. Namai, M. Yumura and S. Iijima, Water-Assisted Highly Efficient Synthesis of Impurity-Free Single-Walled Carbon Nanotubes, *Science*, 2004, **306**, 1362–1364.

26 (*a*) V. Georgakilas, K. Kordatos, M. Prato, D. M. Guldi, M. Holzinger and A. Hirsch, Organic functionalization of carbon nanotubes, *J. Am. Chem. Soc.*, 2002, **124**, 760–761; (*b*) J. L. Bahr and J. M. Tiyr, Covalent chemistry of single-wall carbon nanotubes, *J. Mater. Chem.*, 2002, **12**, 1952–1958; (*c*) I. Kumar, S. Rana and J. W. Cho, Cycloaddition reactions: a controlled approach for carbon nanotube functionalization, *Chem.–Eur. J.*, 2011, **17**, 11092–11101.

27 (*a*) J. L. Bahr, J. Yang, D. V. Kosynkin, M. J. Bronikowski, R. E. Smalley and J. M. Tour, Functionalization of carbon nanotubes by electrochemical reduction of aryl diazonium salts: a bucky paper electrode, *J. Am. Chem. Soc.*, 2001, **123**, 6536–6542; (*b*) A. K. Chakraborty, K. S. Coleman and V. R. Dhanak, The electronic fine structure of 4-nitrophenyl functionalized single-walled carbon nanotubes, *Nanotechnology*, 2009, **20**, 155704.

28 (*a*) J. L. Bahr and J. M. Tour, Highly functionalized carbon nanotubes using in situ generated diazonium compounds, *Chem. Mater.*, 2001, **13**, 3823–3824; (*b*) C. A. Dyke and J. M. Tour, Solvent-free functionalization of carbon nanotubes, *J. Am. Chem. Soc.*, 2003, **125**, 1156–1157.

29 (*a*) M. S. Strano, C. A. Dyke, M. L. Usrey, P. W. Barone, M. J. Allen, H. Shan, C. Kittrell, R. H. Hauge, J. M. Tour and R. E. Smalley, Electronic structure control of single-walled carbon nanotube functionalization, *Science*, 2003, **301**, 1519–1522; (*b*) C. D. Doyle, J.-D. R. Rocha, R. B. Weisman and J. M. Tour, Structure-dependent reactivity of semiconducting single-walled carbon nanotubes with benzenediazonium salts, *J. Am. Chem. Soc.*, 2008, **130**, 6795–6800.

30 N. Nair, M. L. Usrey, W.-J. Kim, R. D. Braatz and M. S. Strano, Estimation of the (*n*, *m*) concentration distribution of single-walled carbon nanotubes from photoabsorption spectra, *Anal. Chem.*, 2006, **78**, 7689–7696.

31 N. Nair, W.-J. Kim, M. L. Usrey and M. S. Strano, A structure-reactivity relationship for single walled carbon nanotubes reacting with 4-hydroxybenzene diazonium salt, *J. Am. Chem. Soc.*, 2007, **129**, 3946–3954.

32 G. Schmidt, S. Gallon, S. Esnouf, J.-P. Bourgoin and P. Chenevier, Mechanism of the coupling of diazonium to single-walled carbon nanotubes and its consequences, *Chem.–Eur. J.*, 2009, **15**, 2101–2110.

33 T. Umeyama, J. Baek, Y. Sato, K. Suenaga, F. A. Chahine, N. V. Tkachenko, H. Lemmetyinen and H. Imahori, Molecular interactions on single-walled carbon nanotubes revealed by high-resolution transmission microscopy, *Nat. Commun.*, 2015, **6**, 7732.

34 Y.-L. Lai, J. Su, L.-X. Wu, D. Luo, X.-Z. Wang, X.-C. Zhou, C.-W. Zhou, X.-P. Zhou and D. Li, Selective separation of pyrene from mixed polycyclic aromatic hydrocarbons by a hexahedral metal-organic cage, *Chin. Chem. Lett.*, 2024, **35**, 108326.

35 For representative reviews of chiral N,N'-dioxides, see:(*a*) W. Cao, X. H. Liu and X. M. Feng, Asymmetric catalytic radical reactions enabled by chiral *N,N'*-dioxide-metal complexes, *Acc. Chem. Res.*, 2025, **58**, 2496–2510; (*b*) D.-F. Chen, L.-Z. Gong and X. M. Feng, Chiral *N,N'*-dioxide ligands uniqueness and impacts, *Org. Chem. Front.*, 2023, **10**, 3676–3683; (*c*) K. Zheng, X. H. Liu and X. M. Feng, Recent advances in metal-catalyzed asymmetric 1,4-conjugate addition (ACA) of nonorganometallic nucleophiles, *Chem. Rev.*, 2018, **118**, 7586–7656; (*d*) X. H. Liu, L. L. Lin and X. M. Feng, Chiral *N,N'*-dioxide ligands: synthesis, coordination chemistry and asymmetric catalysis, *Org. Chem. Front.*, 2014, **1**, 298–302; (*e*) X. H. Liu, L. L. Lin and X. M. Feng, Chiral *N,N'*-dioxide ligands: New ligands and organocatalysts for catalytic asymmetric reactions, *Acc. Chem. Res.*, 2011, **44**, 574–587.

36 (*a*) T. Kitanosono, M. Sakai, M. Ueno and S. Kobayashi, Chiral-Sc catalyzed asymmetric Michael addition/protonation of thiols with enones in water, *Org. Biomol. Chem.*, 2012, **10**, 7134–7147; (*b*) M. Ueno, T. Kitanosono, M. Sakai and S. Kobayashi, Chiral Sc-catalyzed asymmetric Michael reactions of thiols with enones in water, *Org. Biomol. Chem.*, 2011, **9**, 3619–3621; (*c*) S. Bonollo, D. Lanari, F. Pizzo and L. Vaccaro, Sc(III)-catalyzed enantioselective addition of thiols to α,β-unsaturated ketones in neutral water, *Org. Lett.*, 2011, **13**, 2150–2152.